3-2011

Modeling of CFRP-Concrete Interface Subjected to Coupled Pull-out and Push-off Actions

Tayyebeh Mohammadi

Baolin Wan
Marquette University, baolin.wan@marquette.edu

Jian-Guo Dai

Modeling of CFRP-Concrete Interface Subjected to Coupled Pull-out and Push-off Actions

Tayyebeh Mohammadi, Baolin Wan, and Jian-Guo Dai

Synopsis: This paper presents a finite element (FE) modeling method for predicting the IC debonding failure when the FRP/concrete interface is subjected to coupled pull-out (shear) and push-off (dowel) actions. Damaged plasticity model was used to simulate the behavior of concrete close to FRP/concrete interface. A thin damage band exposed to mixed-mode loading condition was modeled separately along the FRP-concrete interface. Cohesive elements were used to model the FRP/concrete interface. A sensitivity analysis was performed to find the appropriate damaged band dimensions, bending stiffness of FRP, and tensile strength of concrete for the model. The numerical results were validated by the experimental data. It was found in this research that the thickness of damage band was not a key parameter when Mode I loading dominated the debonding failure, FRP flexural stiffness had significant effect on behaviors of the strengthened beams, and the concrete tensile strength itself cannot be used as the unique failure criterion for predicting debonding failure.

Keywords: cohesive element, concrete, fiber reinforced polymer (FRP), finite element, mixed-mode loading, plastic damage model

Tayyebeh Mohammadi is a PhD student and research assistant in the Department of Civil and Environmental Engineering at Marquette University. She graduated with a master of science in structural engineering from Ferdowsi University of Mashhad, Iran. Her current research interests include numerical modeling and experimental test of FRP strengthened RC beams.

Baolin Wan is an associate professor in the Department of Civil and Environmental Engineering at Marquette University. He is a member of ACI, an associate member of ACI Committee 440 - Fiber-Reinforced Polymer Reinforcement, and a member of International Institute for FRP in Construction (IIFC). His research interests include numerical and experimental modeling of repaired and retrofitted structures, and durability of FRP repaired concrete structures.

Jian-Guo Dai is an assistant professor in the Department of Civil & Structural Engineering at Hong Kong Polytechnic University. He is a member of International Institution for FRP in Construction (IIFC), International Committee on Concrete Model Code for Asia (ICCMC), and Japan Concrete Institute (JCI). His research interests include strengthening of concrete structures using FRP composites, durability and life cycle management of RC structures in marine environments, and structural applications of fiber-reinforced cementitious composites.

INTRODUCTION

The use of fiber reinforced polymer (FRP) systems as externally bonded reinforcement has become very popular for the repair and strengthening of reinforced concrete (RC) beams as an alternative to the traditional techniques. Extensive researches have been conducted to investigate the behavior of FRP strengthened RC beams experimentally and numerically[1-3]. One of the common failure modes of FRP strengthened RC beams is intermediate crack (IC) debonding of FRP induced by flexural or flexural/shear cracks in the beam. This kind of debonding caused by stress concentration at the tip of flexural or flexural/shear cracks starts at mid-span of beam and propagates along the FRP/concrete interface toward the beam supports as shown in Figure 1. The FRP/concrete interface at the tip of flexural or flexural/shear cracks is subjected to mixed-mode loading compound of dowel action on FRP sheet (Mode I) and shear force along FRP/concrete interface (Mode II) as shown in Figure 1. The dowel action causes tensile stresses acting perpendicular to the interface that make it easier for initial debonding to occur. Therefore, for a proper analysis of IC debonding failure, mixed-mode loading condition along the FRP/concrete interface should be considered.

Finite element analysis has been used to study the behavior of FRP strengthened RC beams[4-8]. Wong and Vecchio[4] used link and contact elements to model the FRP/concrete interface. Monti et al.[5] and Wu and Yin[6] used bi-linear bond-slip models to simulate the

FRP-to-concrete bond. Lu et al.[7] presented a finite element model based on smeared crack approach to predict IC debonding failure. Coronadoa and Lopez[8] performed a sensitivity analysis of reinforced concrete beams strengthened with FRP laminates and found that the fracture energy of the concrete–repair interface is the key parameter for FRP debonding from concrete.

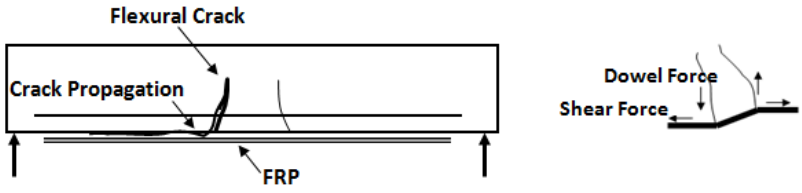

Fig. 1 -- Typical intermediate crack (IC) debonding failure.

Several researches[9-11] have been performed to study the fracture of FRP/concrete interface under mixed-mode loading conditions. Karbhari and Engineer[9] developed a test setup to introduce different interface peeling angles between the FRP sheet and concrete substrate to cause mixed-mode loading at the FRP-concrete interface. Wan et al.[10] used modified double cantilever beam (MDCB) specimens and a customized test frame, which could also introduce different peeling angels, to evaluate the bond characteristics and toughness of FRP bonded concrete under mixed-mode loading. Dai et al.[11] used a beam type of specimen and applied both dowel force and bending load on the beam to create mixed-mode loading at the FRP/concrete interface.

RESEARCH SIGNIFICANCE

In this study, a finite element (FE) modeling method was proposed to predict the IC debonding failure when the interface is subjected to coupled pull-out (shear) and push-off (dowel) actions. According to many researches[9-11], debonding happens in concrete at a small distance from the concrete-adhesive interface and is parallel to the interface. Therefore, a thin damaged band exposed to mixed-mode loading condition was modeled separately along the FRP-concrete interface in the present investigation. A sensitivity analysis was used to find the appropriate damaged band dimensions, bending stiffness of FRP, and tensile strength of concrete for the model. The numerical results were validated by the experimental data.

EXPERIMENTAL BACKGROUND

Dai et al.[11] developed an experimental test setup as shown in Figure 2 to introduce different stress conditions into the FRP sheet to concrete interface through loading the FRP strengthened RC beams in different ways. As shown in Figure 2, a steel bar connected to the loading system was used to impose dowel force vertically onto the FRP sheets through a ball hinge and a stiff plate to create a localized Mode I stress in the FRP-concrete interface. In addition, a steel framework provided reactive bending force to the strengthened RC beams. As a result, the pullout force was introduced into the FRP sheets and a Mode II interfacial stress condition was generated in the FRP/concrete interface. The mixed-mode loading condition could be achieved by altering the dowel force and bending force ratios.

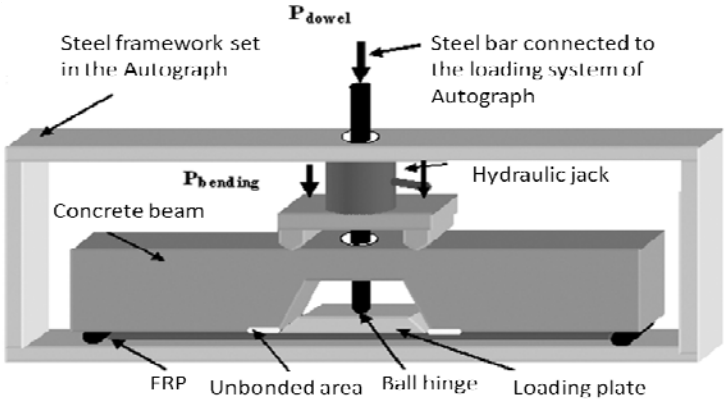

Fig. 2 -- Sketch of test set up[11].

Six RC beams externally bonded with two layers of carbon fiber reinforced polymer (CFRP) sheets had been tested. Dimensions of the specimens are shown in Figure 3. A 20-mm-long initial crack (unbonded area) was set between FRP sheets and concrete beams. Two of six beams subjected to dowel action and bending action only and other specimens were loaded under mixed-mode action by a constant level of dowel force (35%, 50%, 75% and 90% of the interface dowel force capacity) while bending force was increased from zero to the failure loads of the beams. The bending load, dowel load, mid-span deflection, the peeling crack opening displacement, the relative displacement (interfacial slip) between the concrete and CFRP sheet at the starting point of bonding area, and strains in FRP at different locations were measured during tests. More detail of the experimental program can be found in Dai et al.[11]

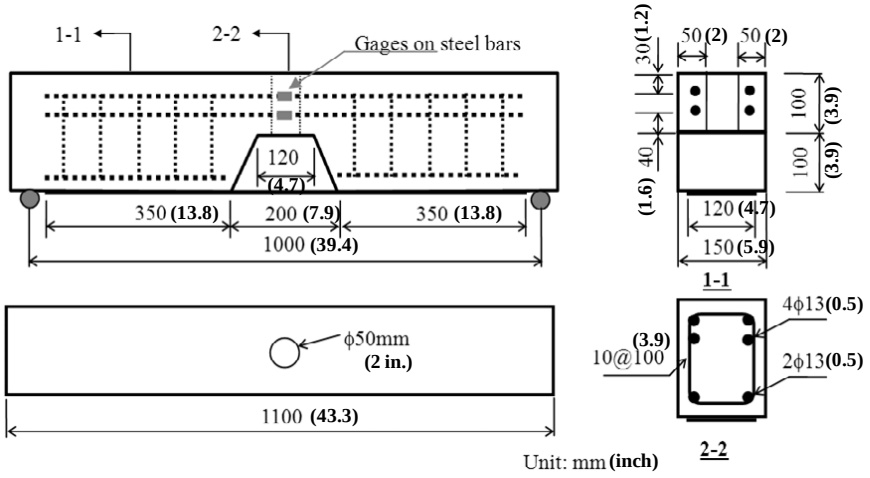

Fig. 3 -- Dimensions of test specimens[11].

All the beams failed due to the peeling of FRP sheets with a thin concrete layer from the substrate. Figure 4 shows the peeled FRP sheets under different loading conditions. There was no significant difference of the volumes of concrete attached to the peeled FRP sheets under different loading conditions. All debonding initiated from the designated unbonded area at midspan. Neither shear cracks nor FRP end debonding were observed. Therefore, this experiment successfully reproduced the interface debonding failure initiating from the mid-span.

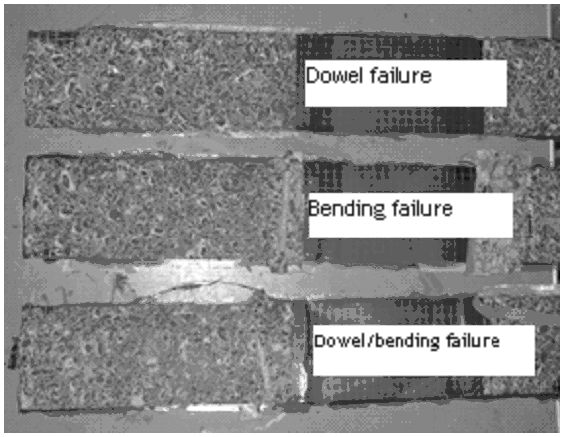

Fig. 4 -- FRP sheets after failure.

CONCRETE DAMAGED PLASTICITY MODEL

Concrete damaged plasticity model is a constitutive model using the concept of fracture energy based damage and stiffness degradation in continuum damage mechanics. It is assumed that the two main failure mechanisms of concrete are cracking in tension and crushing in compression under low confining pressures[12]. This model can describe the nonlinear behavior of concrete including failures in both tension and compression[12,13]. In order to use the concrete damaged plasticity model, two curves should be determined, i.e., softening curve of concrete under tension and stress-strain curve under compression.

Based on the fictitious crack model for fracture of concrete[14], it is assumed that strain localization in uniaxial tension appears only after the maximum load is reached. Therefore, the post peak fracture behavior or softening of concrete can be characterized by a stress vs. crack opening curve as shown in Figure 5. The area under the entire softening stress vs. crack opening curve is denoted as G_F, which is given by

$$G_F = \int_0^{w_c} f'_t dw \tag{1}$$

where f'_t is the softening stress, w is the crack opening displacement, and w_c is the critical crack separation displacement when the softening stress is equal to zero. The material fracture energy, G_F, represents the energy absorbed per unit area of crack and is a material fracture parameter.

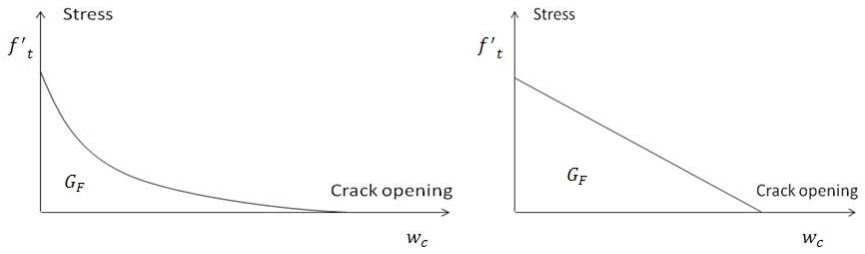

(a) Nonlinear curve (b) Linear approximation

Fig. 5 -- Softening curve of concrete under uniaxial tension.

Equation 1 indicates that the fracture energy, G_F, is related to the shape of the softening curve. Ideally, the curve should be determined by experimental tests for the concrete used in a research. If the actual softening curve is not available, the following equation[15] can be used for estimation of the fracture energy G_F (N/m),

$$G_F = 3.6\left(\frac{f'_c}{0.051}\right)^{0.46}\left(1+\frac{d_a}{11.27}\right)^{0.22}\left(\frac{w}{c}\right)^{-0.3} \tag{2}$$

where f'_c (MPa) is the concrete compressive strength, d_a (mm) is the aggregate diameter, $\alpha_0 = 1.44$ for crushed or angular aggregates, and w/c is the water cement ratio. This equation, which is based on statistical analysis on different test data, can approximately predict the fracture energy of concrete from the standard compression strength, maximum aggregate size, water-cement ratio, and aggregate type[15]. Many different shapes for stress vs. crack opening curves have been proposed[14], such as linear, bilinear, power functions, etc., to simplify the calculation of the fracture energy. In this study, a simple linear stress-crack opening curve as shown in Figure 5(b) was used.

The second curve for the concrete damaged plasticity model is the stress-strain curve under uniaxial compression. The concrete compression stress-strain curve is nonlinear and has different shape for different concrete. In this study, the model proposed by Todeschini et al.[16] as shown in Figure 6 was used to represent the concrete behavior under compression.

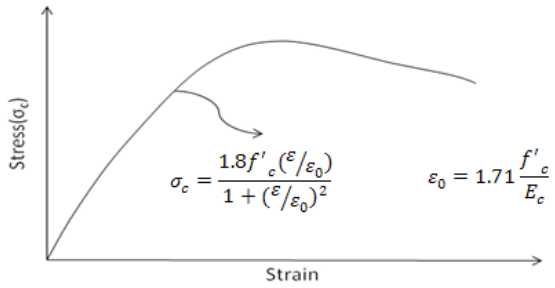

Fig. 6 -- Concrete stress- strain behavior under uniaxial compression[16].

DAMAGED BAND MODELLING

In normal situation, FRP debonding failure happens in concrete which is close to the concrete/adhesive interface as shown in Figure 4. This phenomenon is due to the penetration of adhesive into the concrete and increasing the toughness and the strength of a thin layer of mortar right next to the interface. In this study, a damaged band was created in the FE model to simulate the concrete close to the interface. Cohesive elements were used to model this damaged band.

The cohesive zone ahead of crack tip is shown in Figure 7. In this figure, Δ is the relative displacement between the two surfaces of a crack, and τ is the traction vector. The area under the τ-Δ curve is the fracture energy. Therefore, the fracture energies in different failure mode directions, which are G_{IC} (opening direction) for Mode I, G_{IIC} (in-plane

shear direction) for Mode II, and G_{IIIC} (out of plane shear direction) for Mode III, can be calculated in Equation 3.

$$G_{IC} = \int_0^{\Delta_1} \tau_1 (\Delta_1) d\Delta_1$$

$$G_{IIC} = \int_0^{\Delta_2} \tau_2 (\Delta_2) d\Delta_2 \quad (3)$$

$$G_{IIIC} = \int_0^{\Delta_3} \tau_3 (\Delta_3) d\Delta_3$$

where τ_1, τ_2, and τ_3 are the tractions in Mode I, II and III directions, respectively, and Δ_1, Δ_2, and Δ_3, are relative displacements in Mode I, II and III directions, respectively.

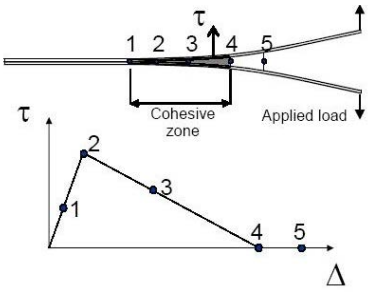

Fig. 7 -- Cohesive zone ahead of crack tip[17].

When the cohesive elements are used to simulate concrete cracking, the onset of cracking is when concrete reaches its ultimate strengths in certain direction, such as tensile strength for Mode I crack. The cracking propagation in each mode is controlled by the fracture energy in that mode.

FINITE ELEMENT ANALYSIS

The finite element analysis software ABAQUS was used for the numerical analysis in this study. Because of the symmetrical condition shown in Figure 3, only half of the beam was modeled. Concrete and FRP were modeled using plain strain element (CPE4R). The steel bars embedded in concrete were modeled using two nodes truss elements (T2D2). The damaged band was modeled using four nodes two dimensional cohesive element (COH2D4). The typical mesh of the model is shown in Figure 8.

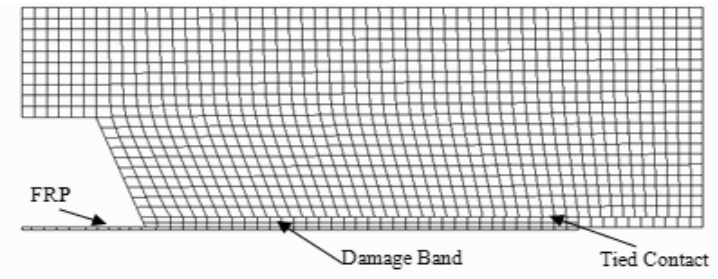

Fig. 8 -- Typical finite element mesh.

Tied contact was used to connect FRP sheet to the damaged band, and the damaged band to the rest of the concrete beam as shown in Figure 8. The tied contact can fuse two regions together even though the meshes created on the surfaces of the regions are dissimilar. In this approach, the nodes on the slave surface have the same displacement as the point on the master surface to which it is closest.

The behavior of steel was modeled as perfectly elastic-plastic response as shown in Figure 9a. The behavior of FRP was modeled using a brittle cracking model as shown in Figure 9b. The stress-strain curve of FRP was assumed to be linearly up to the point when the failure strain was reached and at this point the material lost all its load-carrying capacity suddenly.

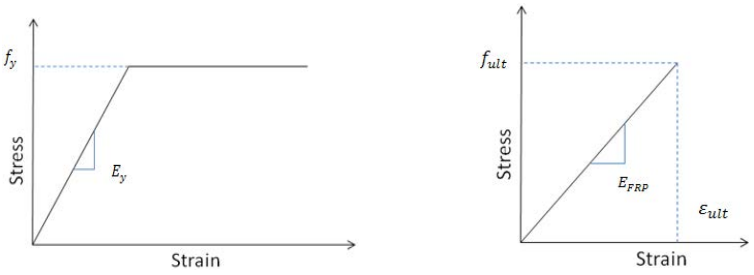

(a) Steel (b) FRP

Fig. 9 -- Stress–strain behaviors used in FE model.

The material properties used in the FE model are presented in Table 1. The damaged band was modeled separately from the rest of concrete beam. The tensile and shear strengths of concrete were assigned to this band to control the initiation of the crack. The critical Mode I and Mode II fracture energies, G_{IC} and G_{IIC}, were assigned to the damaged band in order to predict the mixed-mode crack propagation along the FRP-concrete

interface which was subjected to the coupled pulling and peeling forces. The fracture energies for the interface debonding in these beams were calculated by Dai et al.[11]

Table 1 -- Material properties

Properties	Concrete	Damage Band	FRP	Steel
Modulus of Elasticity E, GPa (ksi)	31.5 (4569)	31.5 (4569)	12 (1740)	210 (30,458)
Yield Strength f_y, MPa (ksi)	-	-	-	575 (83.4)
Tensile Strength, MPa (ksi)	4 (0.6)	4 (0.6)	3550 (515)	-
Compressive Strength f'_c, MPa (ksi)	45 (6.5)	45 (6.5)	-	-
Shear Modulus G, GPa (ksi)	13.12 (1903)	13.12 (1903)	-	-
Shear Strength, MPa (ksi)	1.06 (0.15)	1.06 (0.15)	-	-
Fracture Energy G_F, N/m (lb/ft)	118 (8.1)	G_{Ic} = 610 (42) G_{IIc} = 990 (68)	-	-
Ultimate Strain, %	0.004	0.004	1.5	>0.20
Poisson Ratio	0.2	0.2	0.3	0.3

SENSITIVITY ANALYSIS

Several parameters can affect the FRP debonding failure. In this research, thickness of damaged band, bending stiffness of FRP and concrete strength were selected to study their effects on the IC debonding failure of FRP strengthened RC beams. Two beams, B4 and B6 were chosen to demonstrate the sensitivity analysis of these three parameters. Beam B4 and B6 were subjected to 50% and 90% of its dowel force capacity, respectively[11].

Sensitivity to the thickness of damage band

To find the most accurate damage band thickness for the beams tested by Dai et al.[11], four thicknesses were used in different FE models. They were 2, 4, 7, and 10 mm (0.08, 0.16, 0.28 and 0.39 inches). The load vs. mid span deflection curves for B4 and B9 are shown in Figure 10. The results show that the beam responds were not very sensitive to the damage band thickness although the model with 10-mm-thick of damage band produced the results closer to the experimental data. In the following models, 10 mm (0.39 in.) was used as the thickness of the damaged band.

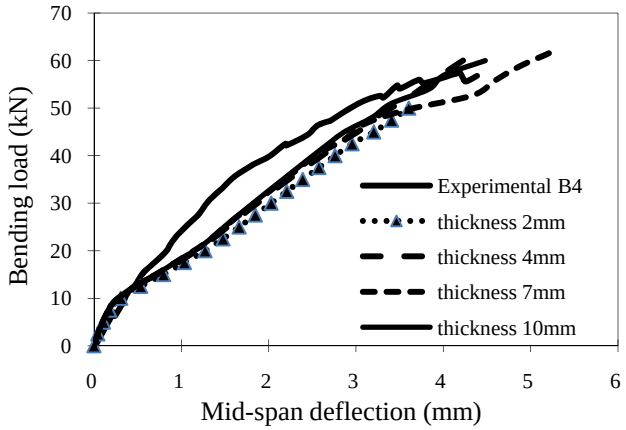

(a) Beam B4 (dowel force was 50% of its capacity).

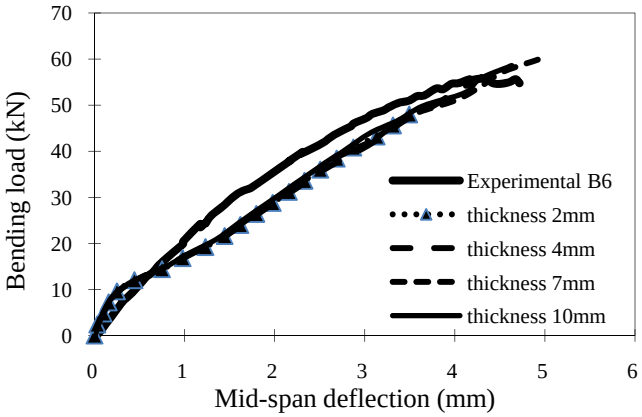

(b) Beam B6 (dowel force was 90% of its capacity).

Fig. 10 -- Sensitivity to the thickness of damage band.
(1mm = 0.039 inch and 1 kN = 0.225 Kips)

Comparison between Figure 10a (dowel force was 50% of its capacity) and Figure 10b (dowel force was 90% of its capacity) indicates that the effect of the damage band thickness was smaller when larger dowel force was applied. Larger dowel force introduced large mode I force to the FRP/concrete interface[11]. Therefore, the thickness of damage band was not a key parameter when Mode I loading dominated the debonding failure.

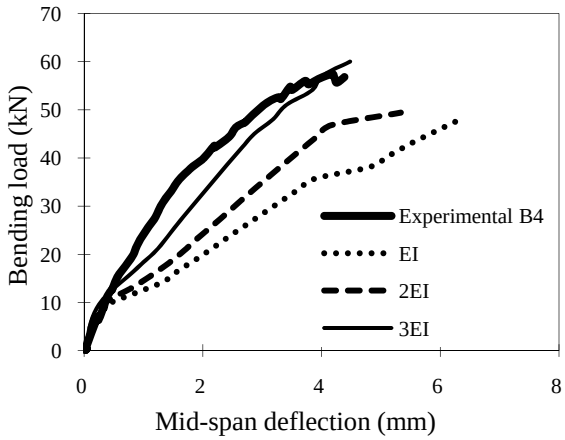

(a) Beam B4 (dowel force was 50% of its capacity).

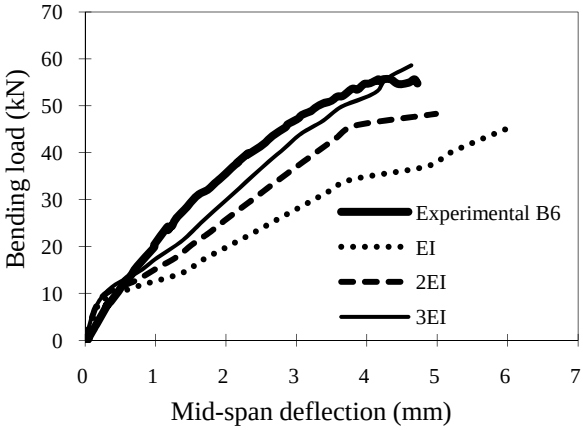

(b) Beam B6 (dowel force was 90% of its capacity).

Fig. 11 -- Sensitivity to the FRP bending stiffness.
(1mm = 0.039 inch and 1 kN = 0.225 Kips)

Sensitivity to the bending stiffness of FRP

In the experimental program, CFRP sheets were applied to RC beam by wet lay-up[11]. The flexural stiffness of CFRP sheet is relatively small and is significantly influenced by the hand layer-up process. Therefore, it is hard to obtain the accurate flexural stiffness of CFRP in the beams. Dai et al.[11] proposed the magnitude of EI = 228000 N·mm^2 (79.4 lb·in^2) for the two layers of CFRP sheets in the beams by using the least-square root regression of the dowel force vs. crack tip opening displacement relationship assuming that the debonded FRP acted as a cantilever beam. Because crack length kept changing

when load was increased (i.e., the length of cantilever beam changed at different loading stages), the slope of dowel force vs. crack tip opening displacement curve might not represent the FRP bending stiffness.

In this study, three FRP flexural stiffness values, i.e., EI, 2EI and 3EI, where EI = 228000 N·mm^2 (79.4 lb·in^2), were chosen to study the FRP flexural stiffness effect on the beams B4 and B6. The numerical results are compared to experimental data as shown in Figure 11. Figure 11 shows that FRP flexural stiffness had significant effect on behaviors of the strengthened beams. The stiffness and ultimate loading capacity of the strengthen beam increased with the increase of FRP bending stiffness. As shown in Figure 11, the bending stiffness of 3EI = 684000 N·mm^2 (238 lb·in^2) had the best agreement with the experimental data. Therefore, 684000 N·mm^2 (238 lb·in^2) was assigned to the FRP bending stiffness in following models.

Sensitivity to the concrete tensile strength

Because debonding failure happened in concrete, it is reasonable to consider the concrete tensile strength as a criterion for the debonding failure at the concrete–adhesive interface[18]. In this study, numerical analyses were performed for beam B4 and B6 with different concrete tensile strengths: $0.5f_t$, f_t and $2f_t$, where f_t is the concrete tensile strength shown in Table 1. The experimental and numerical results of Beam B6 are shown in Figure 12. The FE results show that the higher concrete tensile strength did increase the bending stiffness and ultimate loading capacity of the FRP retrofitted RC beam. However, such improvement was relatively small and the behavior of the retrofitted beam is not very sensitive to the concrete tensile strength. The results of Beam B4 exhibited similar trend. Therefore, the concrete tensile strength itself cannot be used as the unique failure criterion for predicting FRP debonding failure from concrete substrate.

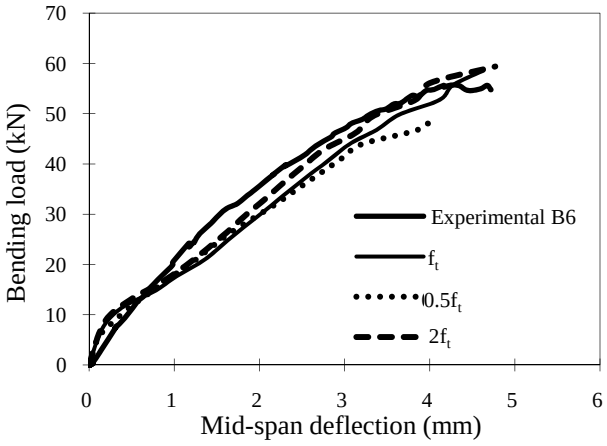

Fig. 12-- Sensitivity to the concrete tensile strength.
(1mm = 0.039 inch and 1 kN = 0.225 Kips)

NUMERICAL RESULTS

Five strengthened beams with IC debonding failure (B2 to B6) were analyzed in FE models by using the parameters discussed in previous sections. The experimental and numerical bending load vs. mid-span curves of B4 are shown in Figure 13. There is a good agreement between numerical and experimental results. Before the preset crack started to propagate, the responds of model and actual beam were almost identical. However, the model shown softer respond after crack propagated. It is due to the characteristics of cohesive element which was used to model the FRP/concrete interface. When the load was increased, the cohesive element continued to deform and therefore the crack propagated continuously in the FE models. In the real beams, the crack stopped at a stable location until the strain energy at the crack tip was accumulated to the fracture energy. Therefore, the crack propagation in the real beam was not continuous. If one observed the experimental curve shown in Figure 13 closely, the curve has see-saw pattern which represents the repeated crack stable and propagating stages. When the crack was stable, the stiffness of the whole beam was high. When crack was propagating, the stiffness of the whole beam dropped. When it reached to ultimate stage, the behaviors of FE model and real beam became similar again. This is because FRP sheets in both model and real beam had debonded completely from concrete in ultimate stage.

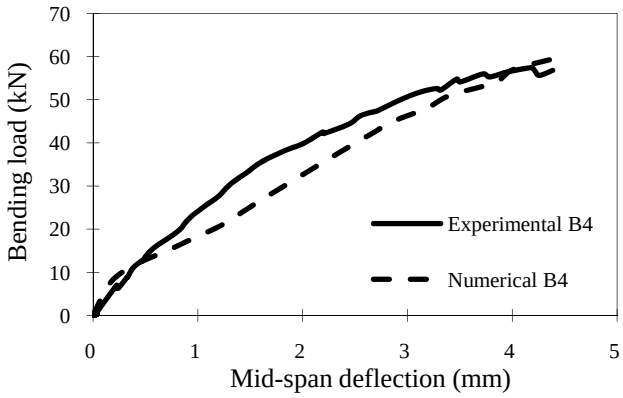

Fig. 13 -- Numerical results against experimental results for load-deflection behavior. (1mm = 0.039 inch and 1 kN = 0.225 Kips)

The peak loads of both numerical and experimental results are presented in Table 2. The maximum error between numerical results and experimental data is 3.5%. These results confirm the validity of the finite element models used in this study.

Table 2 -- Summary of experimental and numerical results.

Beam	P_{dowel}, N (lb)	$P_{bending, max}$, Experimental kN (kips)	$P_{bending, max}$, Numerical kN (kips)
B1	2000 (450)	0	-
B2	0	62 (13.9)	63.6 (14.3)
B3	700 (157)	65.2 (14.7)	62.7 (14.1)
B4	1000 (225)	57.4 (12.9)	60 (13.5)
B5	1400 (315)	53.6 (12.0)	59.4 (13.3)
B6	1900 (427)	55.6 (12.5)	58.6 (13.2)

CONCLUSION

Following conclusions can be drawn from this study.

- The damaged plasticity model and cohesive elements were successfully used to model the behavior of concrete close to interface and the interface crack propagation, respectively. The finite element modeling method used in this study is valid to simulate the FRP strengthened RC beams with IC debonding failure.
- The thickness of damaged band was not a key parameter when Mode I loading dominated the debonding failure.
- FRP flexural stiffness had significant effect on behaviors of the strengthened beams.
- The concrete tensile strength itself cannot be used as the unique failure criterion for predicting FRP debonding failure in FRP strengthened concrete beams.

ACKNOWLEDGEMENT

This research was supported by Marquette University financial aid for graduate student research assistant (RA).

REFERENCE

1. Saadatmanesh, H. and Ehsani, M.R. (1991). ‘‘RC beams strengthened with GFRP plates, Part I: experimental study and Part II: analysis and parametric study”, Journal of Structural Engineering, ASCE, 117(11): 3417-3455.

2. Teng, J.G., Chen, J.F., Smith, S.T. and Lam, L. (2002). “FRP strengthened RC Structures”, John Wiley & Sons, NY.

3. Rahimi, H., Hutchinson, A. (2001). “Concrete beams strengthened with externally bonded FRP plates”. Journal of Composites for Construction, 5(1):44–56.

4. Wong, R. and Vecchio F.J. (2003). “Towards modeling of reinforced concrete members with externally bonded fiber-reinforced polymer composites” ACI Structral Journal, 100(1):47–55.

5. Monti, G., Renzelli, M. and Luciani, P. (2003). “FRP adhesion in uncracked and cracked concrete zones.” Proc., 6th International Symp on FRP Reinforcement for Concrete structures, World Scientific, Singapore: 183–192.

6. Wu, Z.S., Yin, J. (2003). “Fracture behaviors of FRP-strengthened concrete structures” Engineering Fracture Mechanics, 70:1339–1355.

7. Lu, X.Z., Teng, J.G., Ye, L.P. and Jiang, J.J. (2007). ‘‘Intermediate crack debonding in FRP-strengthened beams: FE analysis and strength model’’, Journal of Composites for Construction, ASCE, 11(2):161-174.

8. Coronado, C. and Lopez, M. (2006). “Sensitivity analysis of reinforced concrete beams strengthened with FRP laminates.” Cement & Concrete Composites 28:102–114.

9. Karbhari, V.M. and Engineer, M. (1996). ‘‘Investigation of bond between concrete and composites: use of a peel test’’, Journal of Reinforced Plastics and Composites, 15(2):208-227.

10. Wan, B., Sutton, M.A., Petrou, M.F., Harries, K.A. and Li, N. (2004). ‘‘Investigation of bond between fiber reinforced polymer and concrete undergoing global mixed mode I/II Loading”, Journal of Engineering Mechanics, ASCE, 103(12):1467-1475.

11. Dai, J.G., Wan, B., Yokota, H., and Ueda t. (2009). “Fracture criterion for carbon fiber reinforced polymer sheet to concrete interface subjected to coupled pull-out and push-off actions”. Advances in Structural Engineering, 12(5):663-682.

12. Lubliner, J., Oliver, J., Oller S. and Onate, E. (1989). “Plastic-damage model for concrete” International Journal of Solid Structure, 25 (3):299–326.

13. Lee, J. and Fenves, L.G. (1998). “Plastic-damage concrete model for earthquake analysis of dams” Earthquake Engineering Structure Dynamic, 27(9):937–56.

14. Shah, S.P., Swartz, S.E. and Ouyang, C. (1995). Fracture Mechanics of Concrete: Application of Fracture Mechanics to Concrete, Rock and other Quasi-Brittle Materials, John Wiely & Sons, INC.

15. Bazant, Z.P. and Becq-Giraudon, E. (2002). “Statistical prediction of fracture parameters of concrete and implications for choice of testing standard” Cement Concrete Res, 32(4):529–556.

16. Todeschini, C.E., Bianchini, A.C. and Kesler, C.E. (1964). “Behavior of concrete columns reinforced with high strength steels,” ACI Journal, Proceedings, 61(6): 701-716.

17. Davila, C.G. and Camanho, p.p. (2003). “Analysis of the effects of residual strains and defects on skin/stiffener debonding using decohesion elements,” NASA technical reports, Norfolk, VA.

18. Malek, A., Saadatmanesh, H. and Ehsani, R. (1998). “Prediction of failure load of RC beams strengthened with FRP plate due to stress concentration at the plate end,” ACI Structural Journal, 95(1): 142–152.